

# Theoretical model for predicting the compressive strength of reinforced masonry

## Modelo teórico para a previsão da resistência à compressão da alvenaria armada



R. F. SILVA<sup>a</sup>  
eng\_rfs@hotmail.com

J. S. CAMACHO<sup>b</sup>  
jsc@dec.feis.unesp.br

R. O. RODRIGUES<sup>b</sup>  
ror@dec.feis.unesp.br

### Abstract

This paper compares different models for predicting the compressive strength of concrete block masonry prisms. Four different prism configurations were studied experimentally, each of which was tested without grout (ungROUTED prisms) and with grout and reinforcement (reinforced prisms). The axial compressive strength, strain and failure modes of all the prism configurations were recorded. These results were then compared with different theoretical models for predicting compressive strength, based on the individual strength of each material, its break strain and the strapping effect of the blocks on the system. Among the models studied here, the best results were obtained with those that consider the strapping effect of the concrete block, as well as a change in the break strain of grout.

**Keywords:** structural masonry, concrete blocks, prisms, compressive strength, models.

### Resumo

Neste trabalho faz-se a comparação entre diferentes modelos para se prever a resistência à compressão de prismas de alvenaria de blocos de concreto. Foram estudados experimentalmente quatro tipos diferentes de configurações de prismas, sendo cada um deles ensaiados vazios, ou seja, não grauteados, e preenchidos com graute mais armaduras, denominados prismas armados. Para todos os arranjos de prismas foram registradas as suas resistências à compressão axial, deformações e modos de ruptura. Posteriormente, esses resultados foram comparados com diferentes modelos teóricos de previsão de resistência, baseados nas resistências individuais de cada material, nas suas deformações de ruptura e no efeito de cintamento introduzido pelos blocos no sistema. Entre os modelos estudados, verificou-se que os que conduziram à melhores resultados foram aqueles em que foi considerado o efeito do cintamento proporcionado pelo bloco de concreto e, ainda, uma alteração na deformação de ruptura do graute.

**Palavras-chave:** alvenaria estrutural; blocos de concreto; prismas; resistência à compressão; modelos.

<sup>a</sup> Civil Engineer – PETRÓLEO BRASILEIRO S.A. – PETROBRAS, MSc in Civil Engineering, São Paulo State University (UNESP) – Ilha Solteira School of Engineering, Ilha Solteira/SP, eng\_rfs@hotmail.com, Brazil.

<sup>b</sup> Professor, PhD, Postgraduate Program in Civil Engineering (PPGEC), São Paulo State University (UNESP) – Ilha Solteira School of Engineering, Department of Civil Engineering, jsc@dec.feis.unesp.br, ror@dec.feis.unesp.br, Ilha Solteira/SP, Brazil.

## 1. Introduction

Structural masonry is defined as a component produced on site, consisting of bricks or blocks joined to one another by mortar to form a rigid and cohesive unit. It is a rationalized construction process that has ceased to be undervalued and has become a construction alternative that is competitive from every standpoint. In Brazil, structural masonry stands out for being a highly economic alternative and, compared to conventional concrete buildings, structural masonry concrete blocks show a high potential for growth. However, it should be noted that structural masonry still requires extensive technological improvements to render its performance comparable to that of conventional reinforced concrete structures. The national code, whose main documents of the Brazilian Association of Technical Standards (ABNT) are listed in the references, requires updating, which implies a major effort on the part of research centers to enable the design and construction of economic and safe buildings.

The main components employed in the construction of structural masonry buildings are units (bricks or blocks), mortar, grout and reinforcements (constructive or calculated). As for the materials that make up these units, masonry can be classified as structural masonry of concrete, ceramic, and siliceous limestone blocks. According to Aly [1], concrete blocks emerged in the mid-19<sup>th</sup> century in Europe. Hollow-core concrete blocks, which were created in the United States ca. 1890, soon became popular throughout the U.S. and Europe due to their lightness and satisfactory mechanical strength. This type of concrete block was introduced in Brazil in 1950, when the first machine was imported from the U.S. by the construction company Camargo Corrêa.

According to Page and Shrive [2], the best estimate of the compressive strength of a masonry wall is obtained by testing wall test specimens that are completely representative of *in situ* masonry. However, the testing of walls requires specialized installations and, albeit desirable, such tests cannot be considered suitable routine tests to estimate the strength of a particular unit and mortar combination. Two approximations are usually adopted to estimate the

compressive strength of a masonry wall: (a) tests on individual samples of units and mortar, or (b) tests on small masonry test specimens (prisms or small walls).

Drysdale and Hamid [3], Maurenbrecher [4], Prudêncio Jr. [5], Colville and Wolde-Tinsae [6] and Page et al. [7] state that the results obtained from tests with two-block elements are difficult to correlate with the behavior of the masonry wall. This is because the strapping at the top and bottom of the prism increases its strength and changes its failure mode, hindering its normal failure mode (tension of the units at planes parallel to the applied load) and increasing the load required to break it, thus leading to shear failure. Therefore, tests on prisms should involve at least three units to better represent the wall and minimize the strapping effect imposed by the plates of the press. In tests performed with prisms made of three concrete blocks, the failure mode was found to remain constant, and was characterized by tensile cracking in the central blocks, which is consistent with the failure mode of masonry walls.

In the present study, a comparison was made of different models for predicting the compressive strength of concrete block masonry prisms. Four different prism configurations were tested, each of them without grout (ungrouted prisms) and with grout and reinforcement (reinforced prisms). The axial compressive strength, strain and failure modes of all the prism configurations were recorded. These results were then compared with different theoretical models for predicting compressive strength, based on the individual strength of each material, its break strain and the strapping effect of the blocks on the system.

## 2. Materials and experimental procedure

The test prisms were prepared using only one type of concrete block, mortar and grout. Axial compression tests were performed on the units, the juxtaposed two-block (PR2B) and three-block (PR3B) prisms, bonded prisms PRC1½B (height: 3 courses, length: 1½ blocks) and PRC2B (height: 3 courses, length: 2 blocks), and on ungrouted and reinforced prisms, i.e., prisms containing grout plus reinforcements inside the hollow concrete blocks. Figure 1

**Figure 1 – Arrangement of the test specimens under study: (a) and (b) two (PR2B) and three block prisms (PR3B), respectively, and (c) and (d) stretcher bond prisms (PRC1½B) and (PRC2B), respectively**

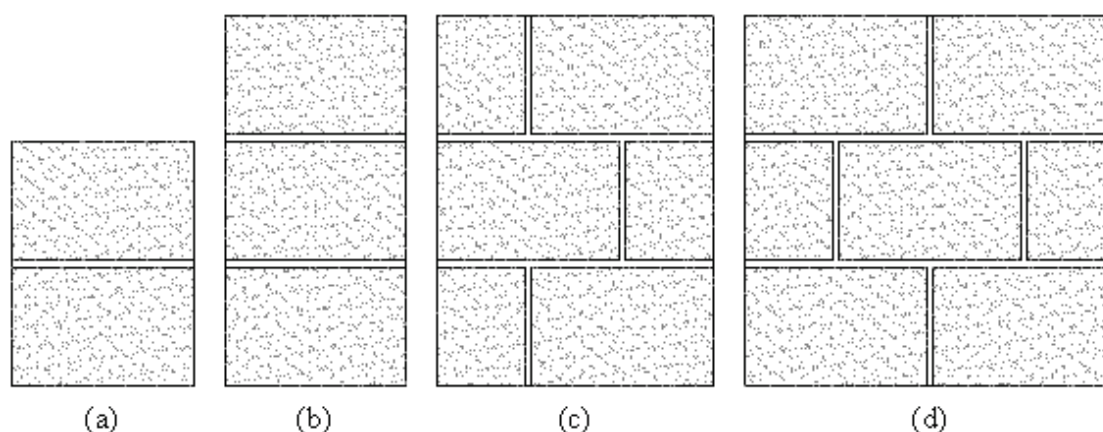
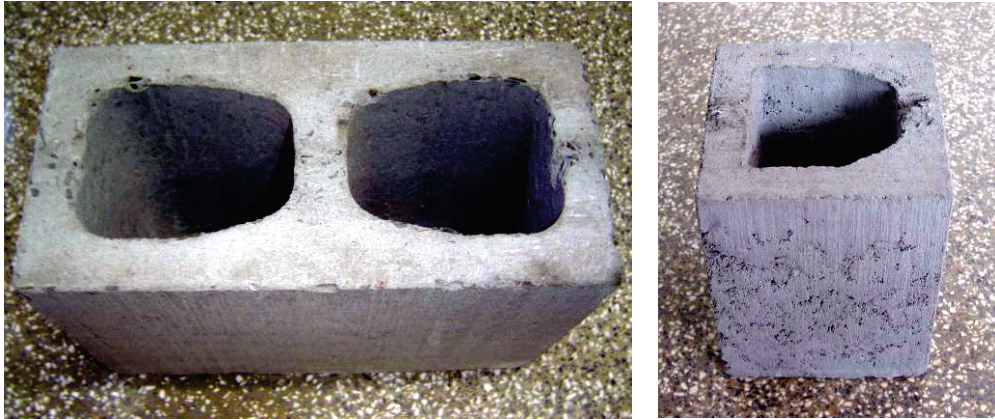


Figure 2 – Concrete blocks used in this study



illustrates the setup of the test specimens, as well as the blocks. The test specimens were analyzed during the tests to evaluate their axial compressive strength and stress strain behavior.

### 2.1 Concrete blocks

Concrete blocks for structural masonry can generally be defined as precast concrete elements made of a suitable mixture of coarse and fine aggregates, cement and water. According to Franco [8], blocks normally represent 80% to 95% of the total masonry, and should therefore meet the basic performance requirements for masonry units, such as mechanical strength, durability, standard dimensions, dimensional tolerance, mass and easy handling, etc. Therefore, it is essential to be familiar with their properties in order to understand the masonry as a whole.

Whole concrete blocks with nominal dimensions of (14x19x29) cm and half blocks with nominal dimensions of (14x19x14) cm (width x height x length) were used (see Fig. 2); however, only the whole blocks were characterized physically to determine their axial compressive strength. The blocks were received in a single lot containing 351 whole blocks and 135 half blocks. With regard to visual characteristics, which may also impair the load-bearing capacity of blocks, the samples exhibited a homogeneous appearance and their live edges were free of cracks and imperfections. The choice of these blocks stemmed from the fact that they are normally used in the construction of buildings of structural masonry, due to their strength and modular dimensions, which are widely available on the market and make it easy to modulate floor plan dimensions.

The blocks were characterized physically based on a dimensional analysis, the water absorption and net area of six test specimens, as described by the Brazilian NBR 12118 standard [9]. Ten test specimens coated with a gypsum layer to ensure the parallelism of their sides and were subjected to an axial compression test, according to the aforementioned standard, using a universal testing machine operating at a rate of 2kN/s, with a loading rate of  $(0.05 \pm 0.01)$ MPa/s in relation to the gross area. This test enabled the determination of the compressive strength of the concrete blocks, i.e., their capacity to bear loads perpendicular to the plane on which they were laid.

### 2.2 Block laying mortar, grout and reinforcements

In masonry, the main function of block laying mortar is to join the units and distribute the stresses uniformly among them. The mortar used in all the tests was prepared with CP II-Z-32 cement, slaked lime and natural siliceous sand, using a mix design of 1:0.75:4.5 (cement: lime: sand), using a mortar joint thickness of approximately 1.0cm between the laid concrete blocks. The mortar components were dry-mixed, achieving an adequate plastic condition and workability with a water/cement (w/c) ratio = 1.14 in mass. This mix design was adopted because it is commonly used in structural masonry construction and also in order to obtain an average strength compatible with that established by the Brazilian NBR 10837 standard [10], which considers that the compressive strength of block laying mortar should be at least 5MPa.

Grout is a micro-concrete composed of a mixture of cement, fine aggregate, coarse aggregate of  $D_{max}=9.5$ cm and water, whose fluidity is suitable for filling the vertical holes of hollow-core concrete blocks. In masonry elements, grout serves to increase the strength of walls, absorbing part of the vertical loads; it confers greater stability to the set, increasing its stiffness, and consolidates the reinforcement to the structure, enabling its positioning. The strength of the grout used in this study was approximately equal to that of the net area of the concrete blocks, and was used in a mix design of 1:1.83:2.17 (cement: sand: gravel) and a w/c ratio of 0.775. Reinforced structural masonry is characterized by having the vertical spaces of the blocks filled with grout that envelops the steel bars. The reinforcement ratio used in the reinforced test specimens was approximately 1% times the gross area of the prism, using 16mm CA-50 steel bars. This ratio corresponds to the use of two steel bars per block, i.e., one bar placed in each hole, in all the test reinforced specimens.

### 2.3 Prisms

The prisms were constructed with the above described components, i.e., units (blocks), mortar and grout. The Brazilian NBR 8215 standard [11] defines an ungrouted prism as a set composed of the juxtaposition of two concrete blocks joined with a mortar joint. Although the Brazilian standards do not mention three-block

Figure 3 - Preparation of the test specimens



prisms, they have been commonly mentioned in studies in which they are employed.

Seventy-two test specimens were prepared and tested under uniaxial compression: 36 ungrouted prisms and 36 reinforced prisms (grout plus reinforcements), making a total of nine test specimens in each configuration. The tested configurations were: two-block (PR2B) and three-block (PR3B) juxtaposed prisms, and bonded prisms of 1 ½ blocks (PRC1½B) and two blocks (PRC2B) three courses in height, coated with a gypsum layer for the axial compression test.

The prisms were prepared and tested under axial compression following the procedures established by the Brazilian NBR 8215 standard [11]. During the preparation of the test specimens, the vertical and horizontal straightness were controlled, and the thickness of the mortar joints was kept at 1.0cm. All the prisms were produced by the same bricklayer, using the same type of mortar, and were laid upon a wooden base to ensure that, albeit exposed to the environment in the laboratory, they would remain protected from sunlight and weathering. Figure 3 shows the setup of some of the tested specimens.

The stress strain behavior of the test specimens was evaluated using LVDTs (Linear Variable Differential Transformers) as displacement measurement devices, to determine the shrinkage of the masonry under incremental loads. Frame brackets were used as

templates to attach the LVDTs with an initial length of L = 20cm for the two-block prisms and of L = 40cm for the three-block and bonded prisms. These brackets were positioned at the vertical holes and at diagonally opposite sides, as illustrated in Figures 4 and 5. All the tests were carried out with the help of a data acquisition system to which the devices were connected. The displacements

Figure 5 - Instrumentation of specimens PR2B, PR3B, PRC1½B and PRC2B, respectively



Figure 4 - Block illustrating the positioning of the LVDTs

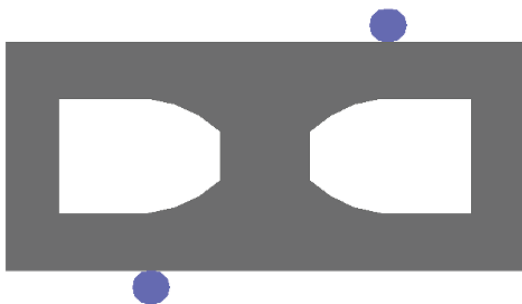


Figure 6 – Instruments employed in this study



Load cell



LVDT



Data acquisition system

of the test specimens measured by the LVDTs, and the variation in load intensity measured by the load cell, were recorded and stored at one-second intervals in a computer, starting from the first instant the load was applied, as indicated in Figures 6 and 7.

### 3. Results and discussion

Based on the Brazilian NBR 12118 standard [9], the blocks were characterized physically by means of a dimensional analysis, water absorption and net area. The results are presented in Table 1, and meet the specifications required by the Brazilian NBR 6136 standard [12]. The axial compression test of the blocks was performed according to the Brazilian NBR 12118 standard [9]. To determine the mean compressive strength, 10 test specimens

Figure 7 – Press used in testing prisms



were tested on a universal testing machine operating at a speed of 2kN/s, following the loading speed of  $(0.05 \pm 0.01)$  MPa/s for the gross area, as specified by the standard. Table 2 lists the results of this test, which indicate the non-occurrence of spurious values with a 95% level of confidence. Failure of the concrete blocks occurred abruptly, with few signs of cracking, which, according to Calçada [13], is the typical failure mode of concrete blocks, as indicated in Figure 8.

In this study only one type of block laying mortar, grout and concrete block were used in all the tests. It should be noted that the purpose here was not to

study the mortar, but the influence of the shape of the test specimens, the grout and the addition of reinforcements on the strength of the masonry. Table 3 shows the mean value of the failure load and the

Table 1 – Mean effective dimensions, absorption and net area of the blocks

Blocks	Width (mm)	Length (mm)	Height (mm)	Gross area (cm <sup>2</sup> )	Absorption (%)	Net area (cm <sup>2</sup> )
Mean	141.72	292.62	189.96	414.69	4.93	283.23
Std deviation	0.35	0.28	1.07	1.32	0.27	5.50
COV (%)	0.25	0.10	0.56	0.32	5.50	1.94

**Table 2 – Axial compression test of the concrete blocks**

CP	Ultimate Load (kN)	Gross area stress (MPa)	Net area stress (MPa)
Mean	577.00	13.91	20.37
Std deviation	105.68	2.55	3.73
COV (%)	-	18.32	-

strength of the mortar and grout at 28 days; during the preparation of the prisms, 12 samples of mortar and grout test specimens were produced. The results of the tests showed a 95% level of confidence (significance of  $\alpha = 0.05$ ) of the non-occurrence of spurious values. It was also found that in all the tests, the failure of the mortar was very similar to the failure load of the test specimens. The axial compression tests of the prisms were performed according to the Brazilian NBR 8215 standard [11], applying a loading

**Figure 8 – Failure mode of concrete blocks**



**Table 3 – Axial compressive strength of mortar and grout**

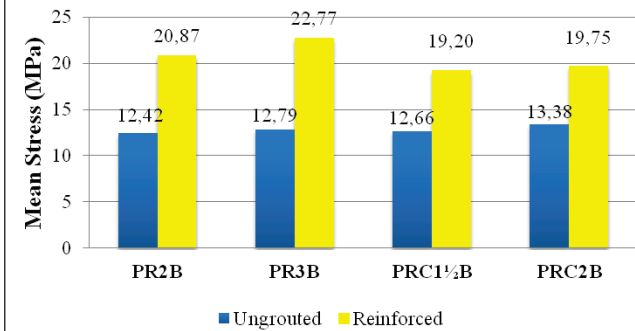
CPs	Mortar Strength (MPa)	Grout Strength (MPa)
Mean	7.89	17.66
Std deviation	0.98	0.86
COV (%)	12.36	4.88

rate of 2kN/s and measuring the shrinkage of the masonry using LVDTs attached to the test specimens. Table 4 lists the values of failure load and stresses of the gross area of the prisms, indicating that the use of grout and reinforcement significantly reduced the coefficient of variation (COV). Figure 9 illustrates the mean strength of the test specimens. The results showed the non-occurrence of spurious values at a 95% level of confidence. All the prisms showed a similar failure mode, which was characterized by the appearance of a main vertical crack in the center of the prism that propagated as the loading increased until it led the prism to rupture. Some reinforced prisms also showed vertical cracks in the grout, mainly in the direction of the reinforcements, as illustrated in Figures 10 and 11. Figure 12 shows the mean stress strain be-

**Table 4 – Axial compression test of the prisms**

TEST SPECIMENS		Ultimate load (kN)		Gross area stress (MPa)		
		Mean	Standard deviation	Mean	Standard deviation	COV (%)
UNGROUTED PRISM	PR2B	515.11	74.00	12.42	1.78	14.36
	PR3B	530.33	90.95	12.79	2.19	17.15
	PRC1½B	787.78	88.58	12.66	1.42	11.24
	PRC2B	1115.00	138.31	13.38	1.66	12.40
REINFORCED PRISM	PR2B	865.56	72.86	20.87	1.76	8.42
	PR3B	944.10	36.64	22.77	0.88	3.88
	PRC1½B	1194.80	95.98	19.20	1.54	8.03
	PRC2B	1646.28	111.76	19.75	1.34	6.79

**Figure 9 – Mean strength of the gross area of the test specimens**



havior of the tested specimens. Insert Figures 10, 11 and 12

#### 4. Models for predicting compressive strength

Different models were proposed to estimate the failure load of the reinforced prisms. In this study, it was considered that the strain measured by the LVDT in the prism was the same as that in the grout and reinforcement, assuming that the materials worked together as a single unit. In the equilibrium equation (1), the values of the parts of the unit can be obtained from the concrete and steel stress-strain diagrams, as shown in Figures 13 and 14.

$$N_S = N_V + N_{GR} + N_{AS} \quad (1)$$

where:

$N_S$  = expected strength of the reinforced prism;

$N_V$  = strength of the ungrouted prism (load obtained in the axial compression tests on ungrouted prisms, for the strain to be analyzed);

$N_{GR} = A_{GR} \times \sigma_{GR}$  (load contributed by the grout);

$A_{GR}$  = area of grout in the prisms (area of the holes of the blocks in the prisms);

$\sigma_{GR}$  = stress in the grout, obtained from the value of the strain in the diagram of Figure 13;

$N_{AS} = A_s \times \sigma_s$  (load contributed by the reinforcement);

$A_s$  = area of reinforcement inserted in the holes of the blocks of the prisms:  $\varphi = 16\text{mm}$ ,  $A_s = 2.01\text{cm}^2$  for each hole of the block;

$\sigma_s$  = stress in the steel, given in Figure 14.

To obtain the results by means of equation (1) and compare them with the experimental values, a maximum failure strain of 2.0‰, which was obtained from the diagram of Figure 13, was first considered and was designated as Model I. It was then considered that the grout would present a maximum strain of 1.5‰, changing the ultimate strain in the expression of Figure 13, as indicated in Figure 16, which was then designated as Model II. Lastly, an increase in the strength of the grout was considered due to the strapping caused by the block and also considering the two ultimate strains mentioned earlier; this was designated as Model III.

The models under study were then subjected to the following procedures:

- The mean values of load vs. strain of the tested prisms were obtained for each test specimen configuration, using the LVDTs.
- Different strains were used with the results of mean load vs. mean strain for the ungrouted and reinforced prisms, as listed in Table 5, and the respective load for verification of equation (1).
- The values of the loads of the ungrouted (UngROUTed  $N_V$ ) and reinforced (Reinforced Experimental) prisms were obtained for a given strain. The value of the theoretical load of the reinforced prism was then determined based on these data and was compared with the experimental value.

**Figure 10 – Failure mode of ungrouted prisms**



Figure 11 – Failure mode of reinforced prisms

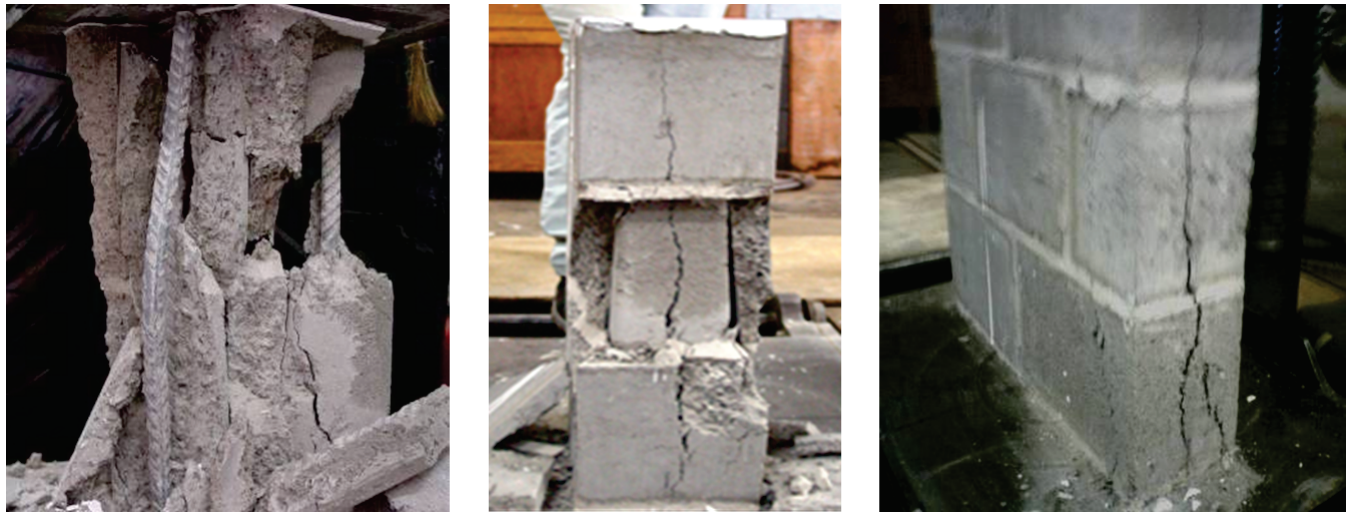
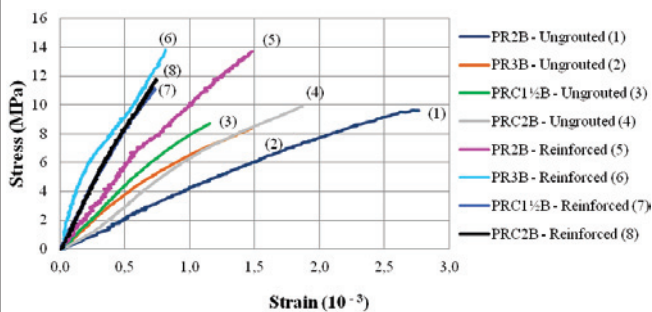


Figure 12 – Mean stress - strain relationship of all the test specimens: ungrouted and reinforced



#### 4.1 Model I

This model considered an ultimate strain of 2.0‰ for the grout obtained from the diagram in Figure 13. The points corresponding to strains of 0.25‰, 0.50‰ and 0.75‰ in the masonry were studied. Equation (1) was checked for different strains, and for the failure load of the reinforced prisms, as shown in Table 6. Because the LVDTs were removed prior to failure of the reinforced prisms to prevent them from undergoing damage due to rupture, tendency lines were inserted in the stress-strain diagram in order to estimate the value of the break strain of these prisms. In Figure 15, the diagram obtained from the tests is shown in thick lines, while the tendency is indicated by thin

Figure 13 – Stress - strain diagram of the grout

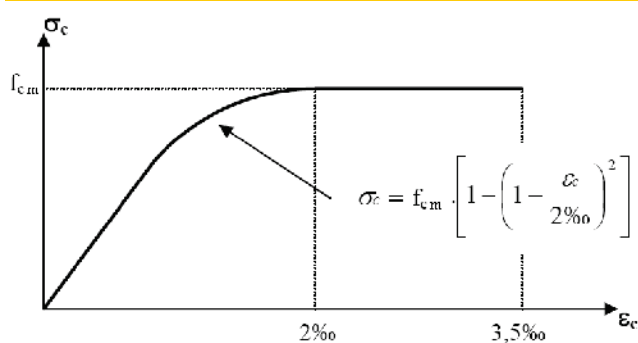
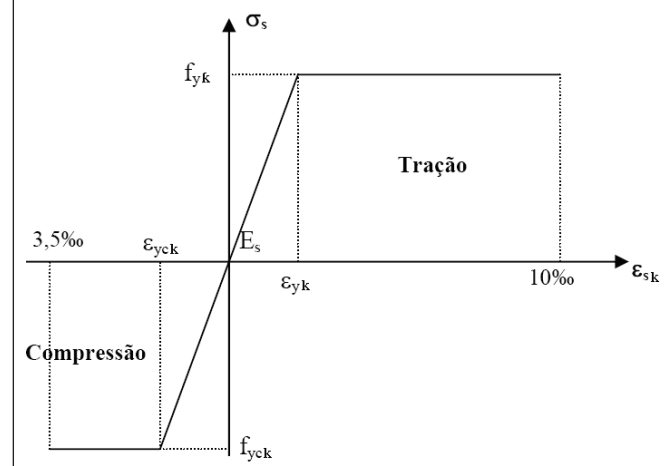


Figure 14 – Stress - strain diagram of the steel

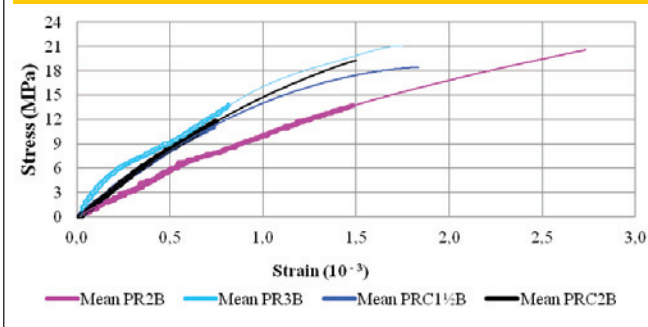


**Table 5 - Comparison of mean theoretical and experimental loads for some of the strains - (Model I)**

LOADS ON THE PRISMS (kN)					
Strain	Test specimens	UngROUTED ( $N_v$ )	Reinforced Theoretical ( $N_s$ )	Reinforced Experimental	Experimental/Theoretical Ratio
$\varepsilon = 0.25\%$	PR2B	37.66	113.18	115.30	1.019
	PR3B	78.31	153.83	261.90	1.703
	PRC1½B	128.21	241.50	279.21	1.156
	PRC2B	97.25	248.30	353.04	1.422
$\varepsilon = 0.50\%$	PR2B	88.18	231.97	240.45	1.037
	PR3B	156.27	300.06	377.42	1.258
	PRC1½B	274.09	489.78	516.33	1.054
	PRC2B	241.41	528.99	689.62	1.304
$\varepsilon = 0.70\%$	PR2B	125.37	318.55	312.68	0.982
	PR3B	207.59	400.77	498.16	1.243
	PRC1½B	372.39	662.17	667.59	1.008
	PRC2B	369.44	755.81	930.19	1.231

**Table 6 - Comparison of mean theoretical and experimental loads for break strain (Model I)**

RUPTURE LOADS OF THE PRISMS (kN)				
Test specimens	UngROUTED ( $N_v$ )	Reinforced Theoretical ( $N_s$ )	Reinforced Experimental	Experimental/Theoretical Ratio
PR2B $\varepsilon = 2.75\%$	397.34	830.56	865.66	1.042
PR3B $\varepsilon = 1.8\%$	320.60	702.44	944.10	1.344
PRC1½B $\varepsilon = 1.8\%$	746.57	1319.33	1194.80	0.906
PRC2B $\varepsilon = 1.5\%$	710.58	1399.21	1646.28	1.177

**Figure 15 - Stress - strain diagram with a tendency line to estimate the break strain of the reinforced prisms**

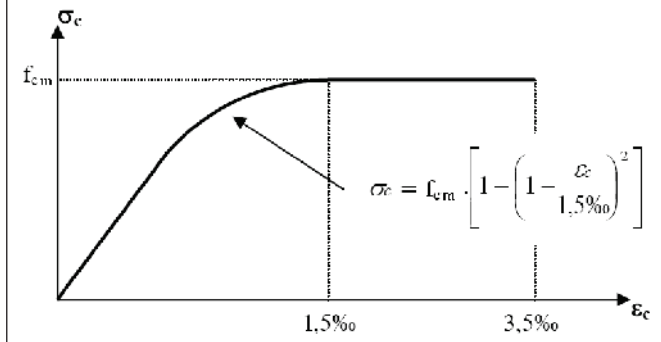
lines, using a 3<sup>rd</sup> order polynomial for the PR2B specimens, a 5<sup>th</sup> order polynomial for the PR3B specimens and a 2<sup>nd</sup> order polynomial for the bonded prisms.

Having determined the estimated break strain and knowing the real failure load of the reinforced prisms, one returns to the proposed equation to find the value of the mean theoretical failure load of these prisms, comparing them with the mean value obtained in the tests. As can be seen, the estimated strains at break of the reinforced prisms were approximately: 2.75‰ for the PR2B specimens; 1.8‰ for PR3B; 1.8‰ for PRC1½B and 1.5‰ for the PRC2B specimens.

#### 4.2 Model II

Tables 7 and 8 were created considering that the grout behaves according to the stress-strain diagram of concrete under a strain of 0 to 2‰. However, the results obtained by Logullo [14] indi-

**Figure 16 - Stress - strain diagram of the grout for  $\epsilon \leq 1.5\text{‰}$**



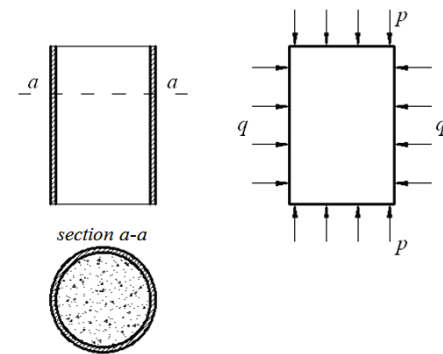
cate that the ultimate strain for concrete blocks with a strength de 15.76MPa and with the same dimensions as the blocks studied here was approximately 1.5‰. Therefore, a change was made in the equation in Figure 13, this time considering a maximum strain of 1.5‰. Hence, the stress in the grout was calculated using the equation shown in Figure 16.

Using this modified equation, Tables 7 and 8 were created for the strains below the break strain and for the estimated strains at break of the reinforced prisms, respectively.

**4.3 Model III**

The equation was also analyzed considering that the grout increases in strength because the block creates a strapping effect, i.e., considering that the strength of the grout increases due to the

**Figure 17 - Concrete cylinder encased in a thin-walled steel pipe**



normal stress caused by the block. The concept of strapped concrete, as well as equation (2), which expresses the increase in load due to the strapping effect, were taken from Santos [15].

**4.3.1 Concept of strapped concrete**

Given a concrete cylinder encased in a thin-walled steel pipe and loaded longitudinally by a force P, the cylinder will undergo longitudinal shrinkage and, due to the Poisson effect, transverse elongation which will be partially hindered by the steel pipe, as shown in Figure 17. Due to the reaction of the pipe, a triple stress state is created in the concrete cylinder and the strength of the concrete increases in relation to the initial fcc strength of the non-strapped concrete.

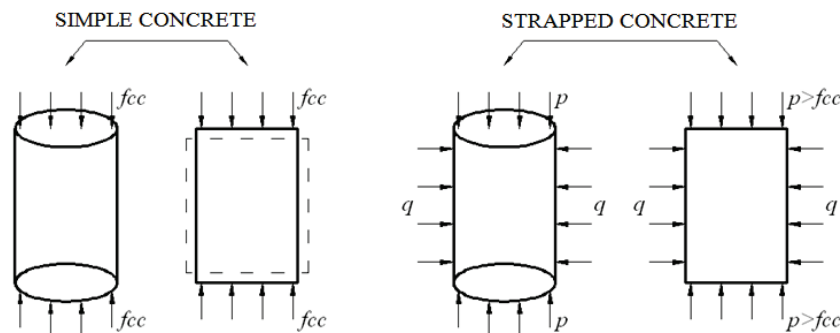
**Table 7 - Comparison of mean theoretical and experimental loads for some strains (Model II)**

LOADS ON THE PRISMS (kN)					
Strain	Test specimens	UngROUTED (N <sub>v</sub> )	Reinforced Theoretical (N <sub>s</sub> )	Reinforced Experimental	Experimental/Theoretical Ratio
ε = 0.25‰	PR2B	37.66	129.71	115.30	0.889
	PR3B	78.31	170.36	261.90	1.537
	PRC1½B	128.21	266.28	279.21	1.049
	PRC2B	97.25	281.35	353.04	1.255
ε = 0.50‰	PR2B	88.18	259.38	240.45	0.927
	PR3B	156.27	327.47	377.42	1.153
	PRC1½B	274.09	530.89	516.33	0.973
	PRC2B	241.41	583.81	689.62	1.181
ε = 0.70‰	PR2B	125.37	350.60	312.68	0.892
	PR3B	207.59	432.82	498.16	1.151
	PRC1½B	372.39	710.24	667.59	0.940
	PRC2B	369.44	819.91	930.19	1.135

**Table 8 - Comparison of mean theoretical and experimental loads for break strain (Model II)**

RUPTURE LOADS OF THE PRISMS (kN)				
Test specimens	UngROUTED (N <sub>v</sub> )	Reinforced Theoretical (N <sub>s</sub> )	Reinforced Experimental	Experimental/Theoretical Ratio
PR2B ε = 2.75‰	397.34	830.56	865.66	1.042
PR3B ε = 1.8‰	320.60	704.76	944.10	1.340
PRC1½B ε = 1.8‰	746.57	1322.81	1194.80	0.903
PRC2B ε = 1.5‰	710.58	1428.23	1646.28	1.153

**Figure 18 - Increase in strength caused by strapping of the concrete**



### 4.3.2 Increase in strength

If the  $f_{cc}$  is the individual strength of a test specimen of simple concrete simples, the strength of the same concrete, when strapped, will be  $p > f_{cc}$ , as indicated in Figure 18.

The new strength of the concrete can be expressed by equation (2):

$$p = f_{cm} + (5 \times q) \tag{2}$$

where:

$p$  = mean value of the strength of the strapped concrete; and  
 $f_{cm}$  = mean value of the strength of the grout.

The value of  $q$  was determined based on the parameters obtained from Figures 19 to 21, which are the geometric characteristics and strengths of the concrete blocks.

Based on Figures 19 to 21, it is possible to obtain the values of the pressures exerted by the grout inside the block in each direction.

$$\text{Direction 1: } q_1 = 2 \times \sigma_{T1} \times (b_1/a) \tag{3}$$

$$\text{Direction 2: } q_2 = 1.5 \times \sigma_{T2} \times (b_2/b) \tag{4}$$

where:

$\sigma_{T1} = \sigma_{T2}$  = tensile strength of the concrete block.

The tensile strength of the block was considered to be the same in the two directions, and with the walls of the block having the same thickness ( $b_1 = b_2$ ) and with  $b > a$ , the lowest value of  $q$  was obtained from equation (4). The results obtained by Albertini [16] for the same blocks indicated that  $\sigma_T \approx 2.75\text{MPa}$ , with  $b_2 = 3\text{cm}$  and  $b \approx 9.5\text{cm}$ . Based on these data and substituting them in equation (4), one has:

$$q_2 = q = 1.5 \times 0.275 \times (3/9.5) = 0.130\text{kN/cm}^2$$

Figure 19 - Plan dimensions of the block; the shaded area is responsible for strapping the grout in the empty cell on the left

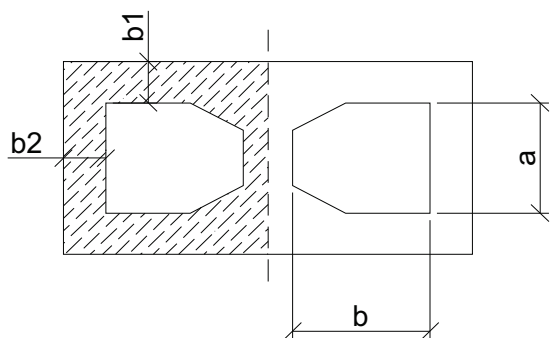


Figure 20 - Possible points of failure of the block walls due to tensile loads

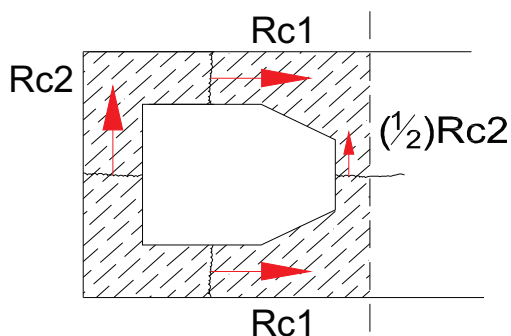
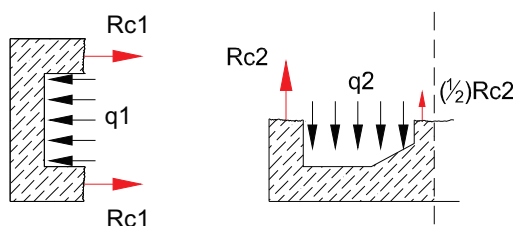


Figure 21 - Resulting pressures on the walls of the blocks in directions 1 and 2



With the value of  $q$  in equation (2), one finds the new value of the compressive strength of the grout, considering the strapping effect. Hence, as can be seen in the calculations below, the mean strength of the grout increases from 17.66MPa to 24.16MPa, i.e., an increase of 37% due to the strapping effect of the concrete block, where:

$f_{cm} = 17.66\text{MPa}$  (Table 3) mean strength of the grout;  
 $p = f_{cm} + (5 \times q) = 1.766 + (5 \times 0.130) = 2.416\text{kN/cm}^2 = 24.16\text{MPa}$   
 Tables 9 and 10 list the results obtained considering the increase in strength provided by strapping, and also the ultimate break strain of the grout of 2.0‰, which is Model III – 2.0‰. Table 9 shows the results obtained considering the strain below the ultimate break strain, while Table 10 lists the results for the estimated break strain of the test specimens.

Similarly to Tables 9 and 10, Tables 11 and 12 lists the results obtained considering the increase in strength caused by strapping, but in this case the ultimate break strain of the grout is 1.5‰, which is Model III – 1.5‰. Table 11 shows the results obtained considering the strain below the break strain, while Table 12 presents the results of the estimated break strain of the test specimens.

Insert Tables 11 and 12

Table 13 summarizes the relationship between the experimental values obtained in the tests and the theoretical values obtained with all the analyzed models for the estimated break strains.

Table 9 - Comparison of mean theoretical and experimental loads for some strains (Model III - 2.0‰)

LOADS ON THE PRISMS (kN)					
Strain	Test specimens	UngROUTED ( $N_v$ )	Reinforced Theoretical ( $N_s$ )	Reinforced Experimental	Experimental/Theoretical Ratio
$\varepsilon = 0.25\text{‰}$	PR2B	37.66	133.21	115.30	0.866
	PR3B	78.31	173.86	261.90	1.506
	PRC1½B	128.21	271.54	279.21	1.028
	PRC2B	97.25	288.35	353.04	1.224
$\varepsilon = 0.50\text{‰}$	PR2B	88.18	269.36	240.45	0.893
	PR3B	156.27	337.45	377.42	1.118
	PRC1½B	274.09	545.85	516.33	0.946
	PRC2B	241.41	603.76	689.62	1.142
$\varepsilon = 0.70\text{‰}$	PR2B	125.37	367.90	312.68	0.850
	PR3B	207.59	450.12	498.16	1.107
	PRC1½B	372.39	736.19	667.59	0.907
	PRC2B	369.44	854.50	930.19	1.089

**Table 10 – Comparison of mean theoretical and experimental loads for break strain (Model III – 2.0‰)**

RUPTURE LOADS OF THE PRISMS (kN)				
Test specimens	UngROUTED ( $N_v$ )	Reinforced Theoretical ( $N_s$ )	Reinforced Experimental	Experimental/Theoretical Ratio
PR2B $\varepsilon = 2.75\text{‰}$	397.34	916.01	865.66	0.945
PR3B $\varepsilon = 1.8\text{‰}$	320.60	787.03	944.10	1.200
PRC1½B $\varepsilon = 1.8\text{‰}$	746.57	1446.22	1194.80	0.826
PRC2B $\varepsilon = 1.5\text{‰}$	710.58	1559.43	1646.28	1.056

**Table 11 – Comparison of mean theoretical and experimental loads for some strains (Model III – 1.5‰)**

LOADS ON THE PRISMS (kN)					
Strain	Test specimens	UngROUTED ( $N_v$ )	Reinforced Theoretical ( $N_s$ )	Reinforced Experimental	Experimental/Theoretical Ratio
$\varepsilon = 0.25\text{‰}$	PR2B	37.66	155.82	115.30	0.740
	PR3B	78.31	196.47	261.90	1.333
	PRC1½B	128.21	305.45	279.21	0.914
	PRC2B	97.25	333.57	353.04	1.058
$\varepsilon = 0.50\text{‰}$	PR2B	88.18	306.85	240.45	0.784
	PR3B	156.27	374.94	377.42	1.007
	PRC1½B	274.09	602.10	516.33	0.858
	PRC2B	241.41	678.75	689.62	1.016
$\varepsilon = 0.70\text{‰}$	PR2B	125.37	411.75	312.68	0.759
	PR3B	207.59	493.97	498.16	1.008
	PRC1½B	372.39	801.96	667.59	0.832
	PRC2B	369.44	942.20	930.19	0.987

## 5. Conclusions

It was found that the values closest to the experimental strains below the break strain were obtained considering the following models: Model I for the juxtaposed two-block prisms (PR2B); Model III (1.5‰) for the juxtaposed three-block prisms (PR3B); Model II for the bonded prisms (PRC1½B), and Model III (1.5‰) for the bonded prisms (PRC2B). Hence, one can see that increasing the number of courses and using bonded test specimens introduces the influence of strapping caused by the block on the grout, thereby reducing the break strain to 1.5‰, as can be observed when passing from PR2B to PR3B and from PRC1½B to PRC2B.

For the break strain, the theoretical values closest to the experimental ones were found by using Model III, for an ultimate strain in the grout of both 1.5‰ and 2‰. However, in general, it can be stated that the results with the lowest errors in rela-

tion to the experimental values were obtained considering an ultimate strain of 1.5‰ in the grout. Therefore, once more, one can see the influence of the normal stress caused by the block on the grout and the reduction of its ultimate break strain to 1.5‰, as was observed with strains below the break strain.

Among the models studied here, the configuration of the prisms (bonded or not) was found to influence the results, and in general, the theoretical results of the bonded prisms were the ones that most closely resembled the experimental results. Thus, it was concluded that for both break strains and lower strains the equation for calculating the stresses in the concrete is valid for calculating the stresses in the grout inserted in the tested prisms, and that the equation should be corrected by the strapping effect caused by the concrete block. Moreover, the addition of grout plus reinforcements was found to significantly reduce the variability of the breaking stresses in the test specimens.

Table 12 – Comparison of mean theoretical vs. experimental loads to break strain (Model III – 1.5‰)

RUPTURE LOADS OF THE PRISMS (kN)				
Test specimens	UngROUTED ( $N_v$ )	Reinforced Theoretical ( $N_s$ )	Reinforced Experimental	Experimental/Theoretical Ratio
PR2B $\varepsilon = 2.75\text{‰}$	397.34	916.01	865.66	0.945
PR3B $\varepsilon = 1.8\text{‰}$	320.60	790.21	944.10	1.195
PRC1½B $\varepsilon = 1.8\text{‰}$	746.57	1450.99	1194.80	0.823
PRC2B $\varepsilon = 1.5\text{‰}$	710.58	1599.13	1646.28	1.029

Table 13 – Relationship between experimental vs. theoretical break strains for all the models

Test specimens	Models			
	I	II	III (2‰)	III (1.5‰)
PR2B	1.042	1.042	0.945	0.945
PR3B	1.344	1.340	1.200	1.195
PRC1½B	0.906	0.903	0.826	0.823
PRC2B	1.177	1.153	1.056	1.029

## 6. Acknowledgments

The authors acknowledge the financial support of the Brazilian research funding agency FAPESP (São Paulo Research Foundation) and thank the company Copel (Araçatuba, SP) for donating the concrete blocks used in this study.

## 7. References

- [01] ALY, V. L. C. Determinação da capacidade resistente do elemento parede de alvenaria armada de blocos de concreto, submetido a esforços de compressão. São Paulo, 1991. Dissertação (Mestrado) - Escola Politécnica de São Paulo, Universidade de São Paulo, 103p.
- [02] PAGE, A. W.; SHRIVE, N. G. A critical assessment of compression tests for hollow block masonry. *Masonry International*, v.2, n.2-2, 1989, p.64-70.
- [03] DRYSDALE, R. G.; HAMID, A. A. Behavior of concrete block masonry under axial compression. *ACI Journal*, v.76, n.6, jun. 1979, p.707-721.
- [04] MAURENBRECHER, A. H. P. Effect of test procedures on compressive strength of masonry prisms. *In: Canadian Masonry Symposium*, 2º, Ottawa, 1980, Proceedings... Ottawa: Carleton University, 1980, p.119-32.
- [05] PRUDÊNCIO Jr, L. R. Resistência à compressão da alvenaria e correlação entre a resistência de unidades, prismas e paredes. Florianópolis, 1986. Dissertação (Mestrado) - Universidade Federal de Santa Catarina, 123p.
- [06] COLVILLE J.; WOLDE-TINSAE, A. M. Compressive strength of grouted concrete masonry. *In: International Brick and Block Masonry Conference*, 9º, Berlim, 1991, Proceedings... Berlim, 1991, v.2, p.149-156.
- [07] PAGE, A. W.; SIMUNDIC, G.; HAN XIE. A study of the relationship between unit, prism, and wall strength for hollow masonry loaded in compression. *In: International Brick and Block Masonry Conference*, 9º, Berlim, 1991, Proceedings... Berlim, 1991, v.1, p. 236-243.
- [08] FRANCO, L. S. Desempenho estrutural do elemento parede de alvenaria empregado na alvenaria estrutural não armada, quando submetido a esforços de compressão. São Paulo, 1987. Dissertação (Mestrado) - Escola Politécnica, Universidade de São Paulo, 136p.
- [09] ASSOCIAÇÃO BRASILEIRA DE NORMAS

- TÉCNICAS. Blocos vazados de concreto simples para alvenaria - Métodos de ensaio. NBR 12118, Rio de Janeiro, 2006.
- [10] ASSOCIAÇÃO BRASILEIRA DE NORMAS TÉCNICAS. Cálculo de alvenaria estrutural de blocos vazados de concreto. NBR 10837, Rio de Janeiro, 1989.
- [11] ASSOCIAÇÃO BRASILEIRA DE NORMAS TÉCNICAS. Prismas de blocos vazados de concreto simples para alvenaria estrutural - Preparo e ensaio à compressão. NBR 8215, Rio de Janeiro, 1983.
- [12] ASSOCIAÇÃO BRASILEIRA DE NORMAS TÉCNICAS. Blocos vazados de concreto simples para alvenaria estrutural - Requisitos. NBR 6136, Rio de Janeiro, 2006.
- [13] CALÇADA, L. M. L. Avaliação do comportamento de prismas grauteados e não grauteados de bloco de concreto. Florianópolis, 1998. Dissertação (Mestrado) - Universidade Federal de Santa Catarina, 188p.
- [14] LOGULLO, B. G. Influência do graute e da taxa de armadura no comportamento da alvenaria de blocos de concreto. Ilha Solteira, 2006. Dissertação (Mestrado) - Faculdade de Engenharia de Ilha Solteira - FEIS, Universidade Estadual Paulista, 192p.
- [15] SANTOS, L. M. Cálculo de concreto armado. São Paulo: Edgar Blucher, 1981, v.2, 458p.
- [16] ALBERTINI, M. M. Análise do comportamento experimental e numérico de prismas de alvenaria estrutural utilizando o elemento finito prismático regular parabólico. Ilha Solteira, 2009. Dissertação (Mestrado) - Faculdade de Engenharia de Ilha Solteira - FEIS, Universidade Estadual Paulista, 208p.